Optimal Generation Scheduling with Dynamic Profiles for the Sustainable Development of Electricity Grids

Carlos Roldán-Blay [1,*] , Vladimiro Miranda [2,3], Leonel Carvalho [2] and Carlos Roldán-Porta [1]

[1] Institute for Energy Engineering, Universitat Politècnica de València, Camino de Vera, s/n, edificio 8E, escalera F, 5ª planta, 46022 Valencia, Spain; croldan@die.upv.es

[2] Institute for Systems and Computer Engineering, Technology and Science (INESC TEC), R. Dr. Roberto Frias, s/n, 4200-465 Porto, Portugal; vmiranda@inesctec.pt (V.M.); leonel.m.carvalho@inesctec.pt (L.C.)

[3] Faculty of Engineering of the University of Porto, R. Dr. Roberto Frias, s/n, 4200-465 Porto, Portugal

* Correspondence: carrolbl@die.upv.es; Tel.: +34-963877007

check for updates

Abstract: The integration of renewable generation in electricity networks is one of the most widespread strategies to improve sustainability and to deal with the energy supply problem. Typically, the reinforcement of the generation fleet of an existing network requires the assessment and minimization of the installation and operating costs of all the energy resources in the network. Such analyses are usually conducted using peak demand and generation data. This paper proposes a method to optimize the location and size of different types of generation resources in a network, taking into account the typical evolution of demand and generation. The importance of considering this evolution is analyzed and the methodology is applied to two standard networks, namely the Institute of Electrical and Electronics Engineers (IEEE) 30-bus and the IEEE 118-bus. The proposed algorithm is based on the use of particle swarm optimization (PSO). In addition, the use of an initialization process based on the cross entropy (CE) method to accelerate convergence in problems of high computational cost is explored. The results of the case studies highlight the importance of considering dynamic demand and generation profiles to reach an effective integration of renewable resources (RRs) towards a sustainable development of electric systems.

Keywords: microgrid planning; optimal generation sizing; optimal generation location; sustainable generation; particle swarm optimization; cross entropy; sustainable development

1. Introduction

Presently there is a global problem of energy supply due to several factors. On the one hand, the scarcity of fossil resources hinders the supply of the power demanded. On the other hand, the environmental impact of greenhouse gas emissions imposes constraints on the use of such technologies [1]. All this implies a high price that is also an obstacle to meet energy needs [2].

The solutions to this problem have been explored for years in various areas. Among them, the development and integration of generators based on renewable resources (RRs) [3] is one of the most promising strategies. These types of generators have some drawbacks, mainly related to their cost and the uncertainty of the generation, but they present a sustainable alternative for the development of electricity grids or the reinforcement of existing networks [4]. Due to the high costs of these systems, feasibility studies to make optimized pre-designs are mandatory. In addition, due to the fact that renewable generation is more fluctuating, these studies are harder compared to the traditional methods based on fixed demand and generation values. If these effects are not taken into account during the

design stage, then the investment plans obtained could be inadequate. The sustainable development of electrical power systems by installing and integrating renewable generators also improves the diversity of energy supply and enables the objectives for addressing climate change approved by most countries to be met [5]. However, despite the aforementioned variable and unpredictable availability of these resources, the methods used to optimize the design of the generation of a network are generally not prepared to be effective and accurate under these conditions [6].

The optimal design of a power grid is a problem of great complexity that involves combining the appropriate selection of topology with the optimal location, size, and operating strategy of generators. Each of these objectives constitutes a complex problem. The optimal design of the generation system in a power grid (location and size of generators) is a non-linear optimization problem that has received considerable attention in recent years. It can be considered a problem with an economic objective (to minimize the cost of generation), like in [7], or as a multi-objective problem, if other criteria are added, such as optimizing voltages in buses or reducing CO_2 emissions, for example [8]. The combinatorial nature of the problem and the mathematical difficulty involved in its solution has often led to evolutionary optimization algorithms, such as particle swarm optimization (PSO), like in [9], or heuristics (genetic algorithms, for example), like in [10–12].

The literature contains many methods for the optimal sizing and placement of generation units in electrical networks, taking into account peak demand and generation values. For example, [13] showed a problem of optimal placement and optimal sizing of distributed generation (DG) in standard networks. The algorithm used for this purpose was PSO. A very similar example can be found in [9]. Like in most research works published in this field, these studies used typical peak values for demand and generation and minimized system losses or costs. Sometimes they also analyzed the improvement in the voltage levels in the network [7], although the method is not designed for that purpose. Other studies have tried to solve the problem using genetic algorithms (GA) [14]. An example that should be highlighted is [15], which is a research work with a comprehensive review of evolutionary methods applied to the optimization of DG. In other works, such as [14] or [16], the optimization of generator placement using GA and fuzzy programming algorithms was explored. In some studies, demand and generation profiles were used in the design process, as in [17], where the installation of a plant in a radial distribution network was optimized, using the same demand profile in all the loads of the network.

This kind of study, based on fixed values for demand and generation, may be fine as an approximation to obtain preliminary solutions, and most research works point in that direction. For example, [18] showed strategies in order to integrate renewable DG and minimize losses. However, these solutions are not optimal in a real situation, where unmanageable generation curves should be considered for each generator. This is especially important for generators based on RRs, such as photovoltaic solar plants or wind farms, since they have great variability [19]. The availability of generation at every instant of time should be used to achieve the optimal solution. Similarly, the evolution of demand along the day should also be considered. This approach is much more realistic than others used in literature [20] and it may provide optimal designs for a network to minimize generation costs over time, considering the variations produced between different moments.

On the one hand, these generation scheduling methods will substantially increase the sustainability of power systems by decreasing their costs and effectively integrate RRs and decreasing greenhouse gas emissions. On the other hand, the difficulty of the problem increases considerably. To the knowledge of the authors, no studies have been developed to solve the generation location and sizing problems at once, with a single method, taking into account both demand and generation profiles. This novel approach provides a much more precise way to schedule generation systems for networks and microgrids.

This article proposes a method based on the use of PSO to optimize the different scenarios obtained when considering generation and demand profiles. The convergence of this metaheuristic in complex problems with large networks may be slow or inadequate for predesigns and feasibility studies. To try to accelerate convergence in complex cases, the initialization of PSO population by using

the cross entropy (CE) method is explored. An example of the use of CE in optimization problems of electric power systems can be found in [21]. Additionally, in the present work, the authors explore a hybrid CE-PSO method for complex, time-consuming problems, where CE is used to provide a guided initialization of the set of particles to run PSO. This analysis is a good starting point for future research. The main contributions of this research work are:

1. The proposed method solves the optimization problems of generation location and sizing in a network simultaneously with a single algorithm;
2. The method produces a significant improvement in the design of the generation mix in a network, thanks to the use of demand and generation profiles in the design process;
3. This work compares the designs obtained with demand and generation profiles with those that result in fixed values of these variables, highlighting the improvements produced by the proposed method;
4. In addition, some results for the improvement of the convergence of the PSO algorithm in cases of high computational cost through a CE-guided initialization are presented.

To illustrate the proposed methodology, two standard Institute of Electrical and Electronics Engineers (IEEE) networks have been adapted. In these networks, realistic demand and generation profiles, obtained through measurements in real facilities, have been assigned to buses. The IEEE 30-Bus system is selected as a base case to conduct an exhaustive analysis of the method and its results. Then, the IEEE 118-Bus system is used as a more complex case to study the improvement in the convergence of PSO algorithm through the initialization by CE. These networks are typical examples for this kind of studies, like in [22].

The paper is structured as follows. Section 2 explains the proposed method and develops the mathematical expressions for its implementation. Section 3 describes the data used for the different case studies. Section 4 shows the results of the simulations and their discussion. Finally, Section 5 shows the conclusions of the study.

2. Materials and Methods

Given a network with n_B buses, the goal was to optimize the location and size of a group of n generators to be installed, so that the generation cost is minimized. Without loss of generality and in order to improve the sustainability of the system, generators based on RRs were considered. It could be assumed that the initial network had n_0 generators, including the connection of a slack bus that was considered bus 1.

Typical demand curves of active and reactive power were known at each bus in the network and maximum and minimum voltage restrictions were considered. The longitudinal and transversal impedances in all the lines were also known.

The set of generators to be added consisted of n_{PV} photovoltaic generators with generation profiles $H_{PV}(t)$, n_W wind generators with generation profiles $H_W(t)$, and n_G manageable generators (which make it possible to fully regulate both active and reactive power generation), such as biogas or hydraulic power plants. Therefore, the total number of generators to be installed was $n = (n_{PV} + n_W + n_G)$ and the total number of decision variables was $2n$. Each pair of decision variables was formed by a first integer one (b_i) with a value in the set $\{2, 3, \ldots, n_B\}$ that represents the bus to which each generator was connected and a second continuous one (s_i) with a minimum value $P_{i_{min}}$ of 0 (although they could have a lower bound greater than 0), which represents the maximum active power installed for each generator. Thus, the vector of decision variables was composed as:

$$x = \left[\begin{array}{ccc} b_1 \, s_1 & \ldots & b_n \, s_n \end{array} \right]_{1x2n}. \tag{1}$$

For each type of generator, the active and reactive power bounds and their typical availability curves were known. For each generator, in each time interval, a generation cost curve was considered according to:

$$C_i(\text{€}) = \alpha_{2_i} \cdot P_i^2 + \alpha_{1_i} \cdot P_i + \alpha_{0_i} + \beta_{2_i} \cdot Q_i^2 + \beta_{1_i} \cdot Q_i. \tag{2}$$

In Equation (2), the variables P_i and Q_i refer to the average active and reactive powers generated, respectively, in each time interval (typically one hour, so the average hourly power and the energy demanded in that hour would be the same). Therefore, C_i is the cost (€) of energy production in each interval. The coefficients α and β define the costs based on the type of generator.

In addition, each new generator to be installed was assigned an amortization cost for each day of C_{a_i} (€/MW). This cost was calculated based on the maximum power that the generator delivered among all the intervals, since it was proportional to the minimum necessary size of each generating plant. Therefore, in this calculation, both active and reactive power generation must be taken into account. For existing generators, amortization could also be considered if the cost and age of each generator was known.

The algorithm should define the bus to which each generator in the set of n generators should be connected and the active power to be installed without exceeding its upper bound $P_{i_{max}}$.

Given a certain vector of decision variables x_a, the network data and the generation curves of each generator were known. Therefore, the optimal power flow (OPF) could be solved by any of the existing algorithms. For this work, the OPF was solved using the Matpower tool in MATLAB [23] and the "fmincon" algorithm of the Matlab Optimization Toolbox, which is designed to find the minimum of non-linear multivariable functions using the interior-point method. The fmincon algorithm calculates the Hessian by a dense quasi-Newton approximation. The basic operation of the interior-point algorithm is briefly described below. For a more detailed description of similar methods for OPF resolution, other works can be explored, like [24–26]. The research work presented in [27] can be highlighted as a comprehensive review of OPF studies applied to smart grids and microgrids with different methods.

The final goal of this problem was to minimize the total generation costs during a typical day. The day was divided into 24 hours. For a typical day, the hourly demand curve of each bus followed a pattern defined by a curve such as those presented in Section 3. Similarly, the generation profiles of photovoltaic or wind generators also follow patterns such as those defined in the same section. If several hours had the same demand and generation data, then they could be grouped in a single scenario k, which allowed the consideration of a total number of scenarios $S \leq 24$ during the day. Consequently, each scenario k took place during h_k hours.

In view of the foregoing, for each vector x_a, considering typical profiles for each consumer and for each generator in the network, such as those proposed in Section 3, the OPF problems in the different scenarios could be solved using the interior-point algorithm. Therefore, the powers $P_i(k)$ and $Q_i(k)$ generated in each generator i could be obtained for each scenario k. Then, the total generation cost could be computed. Finally, the formulation of the OPF problem $\forall k \in [1, S] \cap \mathbb{N}$ was:

$$\min_y C_k(x_a, y) = \sum_{i=1}^{n} \left[h_k \cdot C_{ik} + C_{a_i} \cdot \max_k \left\{ P'_{i,k} \right\} \right] + \sum_{i=n+1}^{n+n_0} \left[h_k \cdot C_{ik} + C_{a_i} \cdot P_{r_i} \right], \tag{3}$$

where $y = \{P_i(k), Q_i(k)\} \; \forall i \in [1, n + n_0] \cap \mathbb{N}$, subject to the following equality constraints $G(x)$:

$$P_{g_i,k} - P_{d_i,k} = \sum_{j=1}^{n_B} U_{i,k} \cdot U_{j,k} \cdot \left(G_{ij} \cdot \cos\left(\theta_{ij,k}\right) + B_{ij} \cdot \sin\left(\theta_{ij,k}\right) \right), \; \forall i \in n_B, \tag{4}$$

$$Q_{g_i,k} - Q_{d_i,k} = \sum_{j=1}^{n_B} U_{i,k} \cdot U_{j,k} \cdot \left(G_{ij} \cdot \sin\left(\theta_{ij,k}\right) - B_{ij} \cdot \cos\left(\theta_{ij,k}\right) \right), \; \forall i \in n_B, \tag{5}$$

and subject to the following inequality constraints $H(x)$:

$$P_{i_{min}} \leq P_{i_k} \leq P_{i_{max}}, \; \forall i \in [1, n + n_0] \cap \mathbb{N}, \tag{6}$$

$$Q_{i_{min}} \leq Q_{i_k} \leq Q_{i_{max}}, \; \forall i \in [1, n + n_0] \cap \mathbb{N}, \tag{7}$$

$$U_{i_{min}} \leq U_{i_k} \leq U_{i_{max}}, \; \forall i \in [1, n_B] \cap \mathbb{N}. \tag{8}$$

In these equations, C_{i_k} is the generation cost of generator i in scenario k; P_{r_i} is the rated power of generator i (which is known for all existing generators in the original network); subscripts d and g refer to powers demanded and generated, respectively; U_{i_k} is the voltage of bus i in scenario k. The values of G and B represent the conductance and susceptance, respectively, in the line that connects two buses, and the angle $\theta_{ij,k}$ is the phase between voltage phasors $\overline{U}_{i,k}$ and $\overline{U}_{j,k}$. In the inequality constraints $U_{i_{min}}$ and $U_{i_{max}}$ are the minimum and maximum voltage limits for bus i, respectively; similarly, $P_{i_{min}}$ and $P_{i_{max}}$ are the minimum and maximum limits of active power generated by generator i, respectively and $Q_{i_{min}}$ and $Q_{i_{max}}$ are the minimum and maximum reactive power limits.

After expressing all inequality constraints as upper bound constraints (changing the sign of lower bound constraints), there were n_i inequality constraints that were converted into equality constraints using a barrier function and a vector of positive slack variables Z. Thus, the problem was modified as follows:

$$\min_y \left[C(y) - \tau \sum_{m=1}^{n_i} \ln(Z_m) \right], \tag{9}$$

subject to:

$$G(y) = 0, \tag{10}$$

$$H(y) + Z = 0, \tag{11}$$

$$Z > 0. \tag{12}$$

The parameter of perturbation τ must be approaching 0 to solve the original problem. Then, for each value of this parameter, the Lagrangian for the equality constrained problem was as follows:

$$\mathcal{L}^\tau(y, Z, \lambda, \mu) = C(y) + \lambda^T G(y) + \mu^T [H(y) + Z] - \tau \sum_{m=1}^{n_i} \ln(Z_m). \tag{13}$$

A feasible interior-point was selected. Then, the partial derivatives and the Hessian of the Lagrangian with respect to y were computed and the problem was solved using a quasi-Newton iterative method by updating the perturbation parameter τ so that it converged to zero.

As a result of the OPF, the active power P_{i_k} and reactive power Q_{i_k} generated by each generator in the network that minimize the generation costs for that scenario were obtained. This process was repeated for each scenario (typically for every hour). According to the demand values at every bus in each scenario, the total generation cost could be obtained by adding the costs of all the generators in the network (both the original ones and those proposed by the vector x_a to be added). Finally, the objective function to be optimized was computed using the following equation:

$$\min C(x_a) = \sum_{k=1}^{S} \left(\min_y C_k(x_a, y) \right). \tag{14}$$

In this equation, $C(x_a)$ is the total generation cost for that typical day in euros with the vector x_a. In that situation, the power to be installed for generator i was $\max_k \{ P\prime_{i,k} \}$. Its calculation was performed using the procedure described below.

For each scenario *k*, the OPF provided the optimum values $P_i(k)$ and $Q_i(k)$ of generator *i*. The minimum necessary power to be installed for that generator was obtained by means of the following equation:

$$\max_k\left\{P'_{i,\,k}\right\} = \max_k\left\{\max\left\{\frac{P_i(k)}{H_i(k)}, \frac{Q_i(k)}{H_i(k)\cdot tg(\varphi_i)}\right\}\right\} \leq P_{i_{max}}. \tag{15}$$

In this equation, $H_i(k)$ is the typical utilization coefficient of generator *i* in scenario *k*, according to its generation curve and φ_i is the typical power angle of that generator. Therefore, this calculation corresponded to the minimum power to be installed for generator *i* to be able to supply the necessary active and reactive power according to the OPF result.

Once the minimum cost for the vector x_a was obtained, it was necessary to modify it to cover all possible combinations of its variables. Taking into account the enormous number of possibilities that this represents, the use of the PSO algorithm was proposed to solve the problem of minimizing the global cost $C(€)$. This algorithm is described below.

A sample consisting of χ particles was chosen. The position of each particle corresponded to a vector x_i. The initial positions of the particles were taken uniformly distributed, trying to cover the entire space of feasible values of every decision variable. In each iteration, each particle obtained a value of the objective function and its best value throughout the algorithm (local best) was stored. In each iteration, the global best value of the objective function so far (global best) was also updated. Typical stop criteria may be the number of iterations or tolerance (small changes in global best).

The steps of PSO algorithm in each iteration were as follows:

1.　Evaluate the value of the objective function of each particle at the current position $C(x_i)$;
2.　Update the individual best value of the objective function for every particle (local best) and the global best value of the objective function for the entire population (global best);
3.　Update the velocity of each particle and get its new position for the next iteration.

In each iteration *t*, the position of every particle *i* of the sample was updated using the following equation:

$$x_i^{(t+1)} = x_i^{(t)} + v_i^{(t+1)}, \tag{16}$$

where *x* is the position and *v* is the velocity of the particle. Velocities must be calculated as:

$$v_i^{(t+1)} = \vartheta\cdot v_i^{(t)} + c_1\cdot r_1\cdot\left(\hat{x}_i^{(t)} - x_i^{(t)}\right) + c_2\cdot r_2\cdot\left(g^{(t)} - x_i^{(t)}\right), \tag{17}$$

where *i* is the particle index, ϑ is the inertial coefficient, c_1 and c_2 are acceleration coefficients ($0 \leq c_1, c_2 \leq 2$), r_1 and r_2 are random values ($0 \leq r_1, r_2 \leq 1$) regenerated before every velocity update, $v_i^{(t)}$ is the particle's velocity at iteration *t*, $x_i^{(t)}$ is the particle's position at iteration *t*, $\hat{x}_i^{(t)}$ is the particle's individual best solution until iteration *t* and $g^{(t)}$ is the swarm's best solution until time iteration *t*.

If the network was very large (for example, $n_B > 50$), then the computation cost was very high. To make a quick pre-design, the initial population for PSO could be initialized by means of a few iterations of the CE algorithm (for example, four iterations). Four iterations of CE provided a better guided set of particles, which also made it possible to reduce the number of particles for PSO. The second case study was selected to explore this option and some results are included in the results and discussion section.

The CE algorithm used for optimization is described below:

1.　Select an initial sample of *N* uniformly distributed random particles $\{X_1, \ldots, X_N\}$. Each particle represents a vector of decision variables $X_a = [X_a(d)]_{d=1}^{2n}$;
2.　Select the rarity parameter (elitist population ratio) ρ and smoothing parameters γ and δ;

3. Calculate $\mu_{0,d}$ and $\sigma_{0,d}^2$, mean value and variance of each decision variable in the population using the following expressions:

$$\mu_{0,d} = \frac{1}{N} \sum_{i=1}^{N} X_i(d), \tag{18}$$

$$\sigma_{0,d}^2 = \frac{1}{N-1} \sum_{i=1}^{N} \left(X_i(d) - \mu_{0,d}\right)^2; \tag{19}$$

4. Initialize the iteration counter $h = 1$;
5. Perform an iteration with the following steps:

   a. Compute the objective function of each particle $\{C(X_1), \ldots, C(X_N)\}$;
   b. Sort all particles from best to worst;
   c. Select N_{elite} particles as the best ρ fraction of the sorted particles;
   d. Assuming a Gaussian distribution, calculate the distribution parameters for each variable:

$$\mu_{h,d} = \frac{1}{N_{elite}} \sum_{i=1}^{N_{elite}} X_i(d), \tag{20}$$

$$\sigma_{h,d}^2 = \frac{1}{N_{elite}-1} \sum_{i=1}^{N_{elite}} \left(X_i(d) - \mu_{h,d}\right)^2; \tag{21}$$

   e. Apply smoothing parameters:

$$\mu_{h,d} = \gamma \cdot \mu_{h,d} + (1-\gamma) \cdot \mu_{h-1,d}, \tag{22}$$

$$\sigma_{h,d}^2 = \delta \cdot \sigma_{h,d}^2 + (1-\delta) \cdot \sigma_{h-1,d}^2; \tag{23}$$

   f. Generate a new random sample with a Gaussian distribution using $\mu_{h,d}$ and $\sigma_{h,d}^2$;
   g. Finish iteration $h = h + 1$;

6. If $h \leq h_{max}$, then repeat step 5. Otherwise, end.

For a more detailed explanation of the CE method, other texts can be explored. Among them, [28] should be highlighted due to the exhaustive explanations and examples that it contains.

The proposed method, which was called Optimal Generation Scheduling with Dynamic Profiles (OGSDYP), is summarized in Figure 1.

The main focus of the OGSDYP method is that dynamic profiles should be used to define loads and generators in order to achieve accurate results. The steps to perform a simulation with the method are explained below.

1. Grid data collection (grid structure and parameters). The typical profiles for every load and every existing generator must be used in the simulation process;
2. New generators definition. The maximum number of generators of each type to be installed, their maximum size, and their costs must be defined. Generator profiles must be included;
3. Use PSO to optimize the location (integer variables) and size (continuous variables) of each new generator. This algorithm will provide the nodes and rated power of each new generator. If a generator is not needed, it will be assigned 0 kW;
4. During PSO, every particle provides a proposal of generation schedule. Then, for every instant of the typical day, the proposed schedule must be optimally managed to determine the minimum cost of every particle. This is performed using interior-point algorithm to calculate every OPF;

5.　By combining generator profile and the power supply scheduled for every hour, the optimal size of every new generator is computed and the objective function value of every PSO particle is calculated;

6.　A new set of particles is generated to continue with PSO algorithm until convergence is reached.
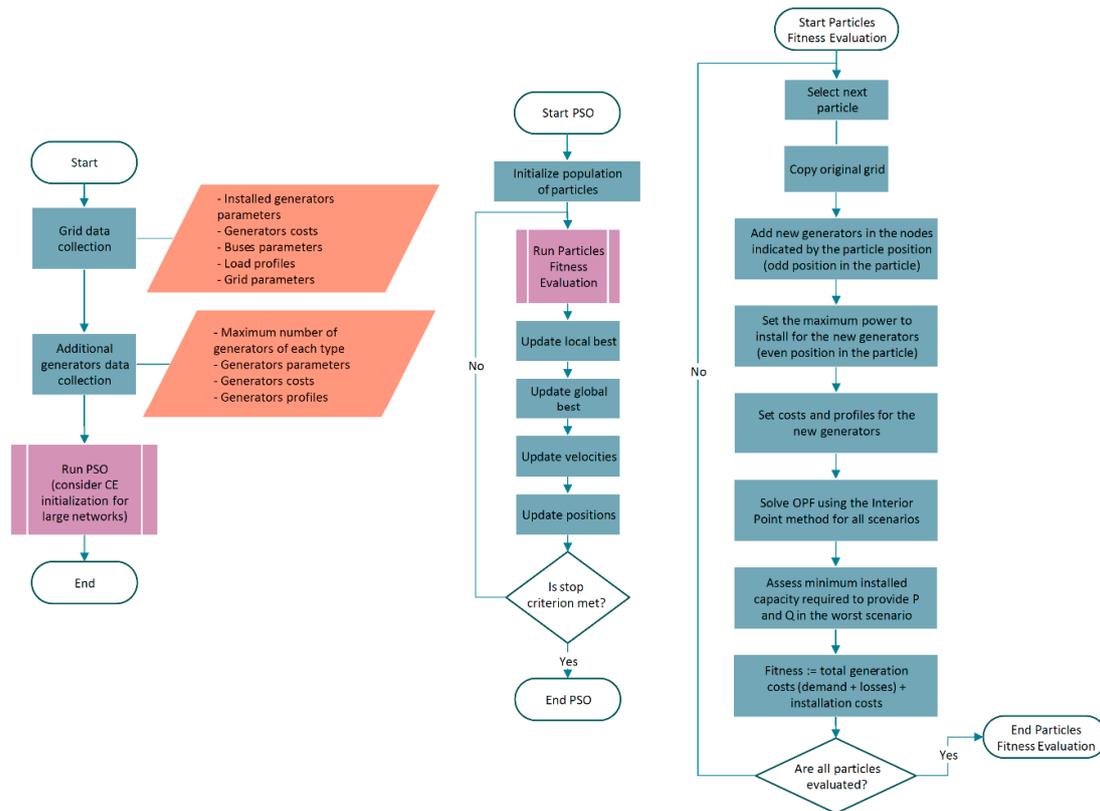

Figure 1. Diagram of the Optimal Generation Scheduling with Dynamic Profiles (OGSDYP) method.

Using the proposed method, some of the drawbacks of the previously published methods in the literature are solved. Thus, the main advantages of the OGSDYP method can be summarized as follows:

1.　The use of a single method (a single simulation) to optimally schedule generation facilities. Most methods use one algorithm to find the optimal types and location for generators and a different one to calculate the optimal sizes [9]. Others calculate the optimal sizes in a combination of nodes, exploring all possible locations by brute force algorithms [7]. In the proposed method, if the set of generators is big enough, the OGSDYP method will provide information on which generators to install (how many of each type), in which nodes, and with which size;

2.　The use of dynamic profiles for each generator and each load. Most methods use fixed values, typically average (AVG) or peak values, of active and reactive power in every node [7,9,13]. As the 30-bus system will demonstrate, this may lead to huge differences in total costs in real operating conditions. Other works use curves only for demand facilities or only for generators. Some recent studies use a single demand profile in all nodes in distribution networks [17]. The proposed method can be applied with different demand profiles of active and reactive power at every node and with different availability profiles for each generator, depending on the type and the geographical location of each power plant. Thus, it is a much more realistic method, with better results, as proven with the case studies. Also, the method may take into account the installation costs of each new generator and the costs of reactive power production, not considered in many

previous studies [20]. Therefore, it includes all advantages of the previous works and provides some new benefits related to accuracy, simplicity, and optimality.

Just as an example to show the complexity of the method and with the purpose of clarifying the usage of every algorithm, let us assume that 25 particles are used in PSO, 20 iterations are performed, and 24 time intervals are considered in the typical day. In this situation, PSO will evaluate the objective function a total of $25 \times 20 = 500$ times, and $500 \times 24 = 12,000$ OPF problems will be solved using the interior-point method. Due to this reason, the OGSDYP method involves high computational costs, especially in large networks. This is the reason why the authors highlight the need to develop future research focused on accelerating the convergence of PSO in large networks. Just as an experimental proposal, the authors tested CE initialization in a large network and the results are shown in the second case study. Although the results are not conclusive, this is an interesting starting point for future research.

3. Case Studies

Two standard networks were adapted to test the proposed method. The first one was the IEEE 30-Bus system and the second one was the IEEE 118-Bus system. In each case, the standard network was taken, while maintaining the slack bus generator, to optimize the location and size of the generation to be installed. Some installed generators present in the original network may be considered. However, in the IEEE 30-Bus system, all the previous existing generators were removed, leaving the slack bus as the only initial generator. This ensured that the proposed solution will consist of a set of new generators with high installed powers, which will illustrate the method performance and facilitate the analysis of the results. The slack bus was modeled as a network from which any amount of energy can be imported, but not exported. This was done because if exportation is allowed, then the algorithm can oversize the generators and take advantage of the exportation economically, thus resulting in non-realistic scenarios. The definition of these case studies was made to illustrate the application of the method and the possibilities it offers by analyzing the obtained results. In studies with real networks, the exportation of energy can be considered, taking into account the selling price of energy, as well as adjusting the costs assigned to each generator with real prices for each case. The demand and generation curves obtained to develop these case studies can also be modified. Moreover, specific curves could be assigned to each bus to take into account the geographical position of generators and the influence on their availability.

For each selected network, a classification of the types of consumers in the buses was proposed, taking into account the peak powers demanded in the original case according to the procedure explained below. This procedure was carried out in order to demonstrate the effectiveness of the proposed optimization algorithm for different demand curves in the buses.

The maximum active power demand in the original network was modified using a curve assigned to each bus based on the percentile to which each demand value belonged, according to Table 1. Thus, the proposed assignment was the result of analyzing the demands of the original network and classifying them into four groups based on their size.

Table 1. Considered demand profiles.

Percentile	Type of Curve	Type of Consumer	Example
No demand	-	None	-
(0% ÷ 16%)	H_1	Small consumer	Residential area with low population density
(16% ÷ 36%)	H_2	Medium consumer	Residential area with high population density
(36% ÷ 71%)	H_3	Large consumer	Area with large number of industrial and services buildings
(71% ÷ 100%)	H_4	Very large consumer	Large urban centers

For each type of consumer, the average scaled curve of consumers of that type was used based on actual measurements or real data obtained for this study. Reactive power curves were obtained from the measured active power curves and the typical power factor of the buses where these demand profiles were placed in the original network. Similarly, reactive power limits were considered in generators based on the typical power factor of each type of generator.

The different groups of consumers considered and the assigned curves are described below. The availability curves of solar and wind power plants are also shown according to real data.

3.1. Small Consumer

The average hourly active power of a block of 20 homes and a set of five buildings of a university campus used for commercial and service areas was measured for one year. Figure 2 shows the average curves during the measurement campaign in per unit values H_1 represented with bars and their standard deviation Hsd_1 represented with a line, calculated with Equation (24). This equation considered a sample of N days, where v_{j_i} is the value of the hourly energy of day j at hour i in per unit values (compared to the maximum registered value) and μ_i is the average value for that hour. For this curve, its daily average value $AVG_1 = 0.284$ was also obtained, using Equation (25), and its root mean square value $RMS_1 = 0.320$, using Equation (26).

$$Hsd_i = \sqrt{\frac{1}{N-1}\sum_{j=1}^{N}\left(v_{j_i} - \mu_i\right)^2}, \tag{24}$$

$$AVG = \sum_{k=1}^{S} h_k \frac{v_k}{S}, \tag{25}$$

$$RMS = \sqrt{\sum_{k=1}^{S} h_k \frac{v_k^2}{S}}. \tag{26}$$
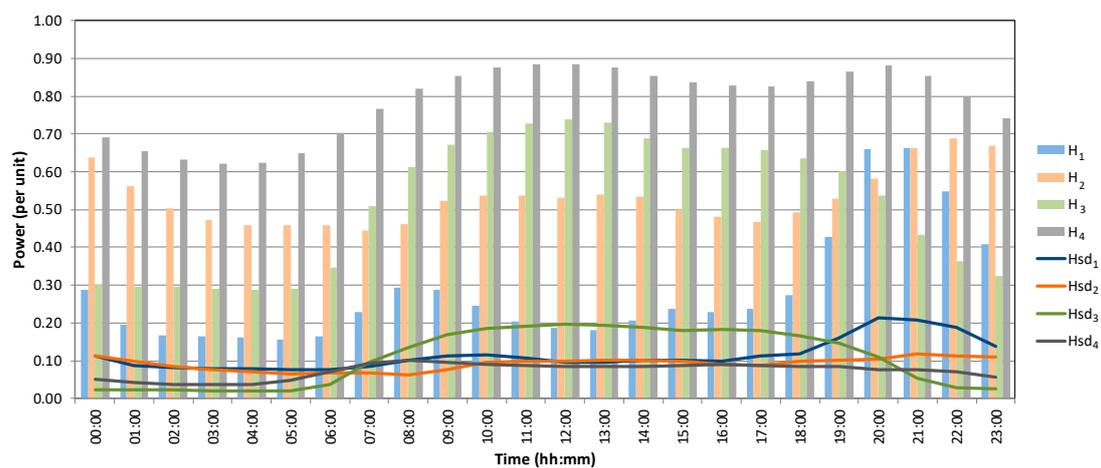
Figure 2. Demand profiles considered in the case studies.

That is, if a bus classified as a small consumer has a maximum registered demand of $\hat{p}$ in the original network, its average demand at each hour t of the day would be:

$$P(t) = \hat{p} \cdot H_1(t). \tag{27}$$

3.2. Medium Consumer

The average hourly active power demand of a municipality in Spain with a population of about 500 inhabitants was measured for one year. Figure 2 shows the average curves during the measurement campaign in per unit values H_2 represented by bars and their standard deviation Hsd_2 represented by a line. For this curve, an average value of $AVG_2 = 0.530$ and a root mean square value of $RMS_2 = 0.535$ were obtained.

3.3. Large Consumer

The average hourly active power of an administrative, university, and commercial complex with about 90 buildings and a peak power exceeding 16 MW was measured for several years. Figure 2 shows the average curves for a whole year of the measurement campaign in per unit values H_3 represented with bars and their standard deviation Hsd_3 represented with a line. For this curve, the average value $AVG_3 = 0.516$ and the root mean square value $RMS_3 = 0.544$ were obtained.

3.4. Very Large Consumer

The demand curves of the Spanish electricity system were obtained for one year from the system operator website [29]. The average curves during the selected period are shown in Figure 2 in per unit values H_4 represented by bars and their standard deviation Hsd_4 is represented by a line. For this curve, its average value $AVG_4 = 0.786$ and its effective value $RMS_4 = 0.791$ were obtained.

3.5. Photovoltaic Generation

For generation, the curves of the generators to be installed were also analyzed. The average hourly active power generated by a set of 10 photovoltaic solar plants was measured for one year. These plants were approximately located on the latitude line 40°N and the longitude line 1.5°W. Figure 3a shows the average curves during the measurement campaign in per unit values H_{PV} represented by bars and their standard deviation Hsd_{PV} represented by a line. For this curve, an average value of $AVG_{PV} = 0.239$ and a root mean square value of $RMS_{PV} = 0.384$ were obtained. In these generators the power factor will be assumed to be 1.00, so that they cannot provide nor consume reactive power.
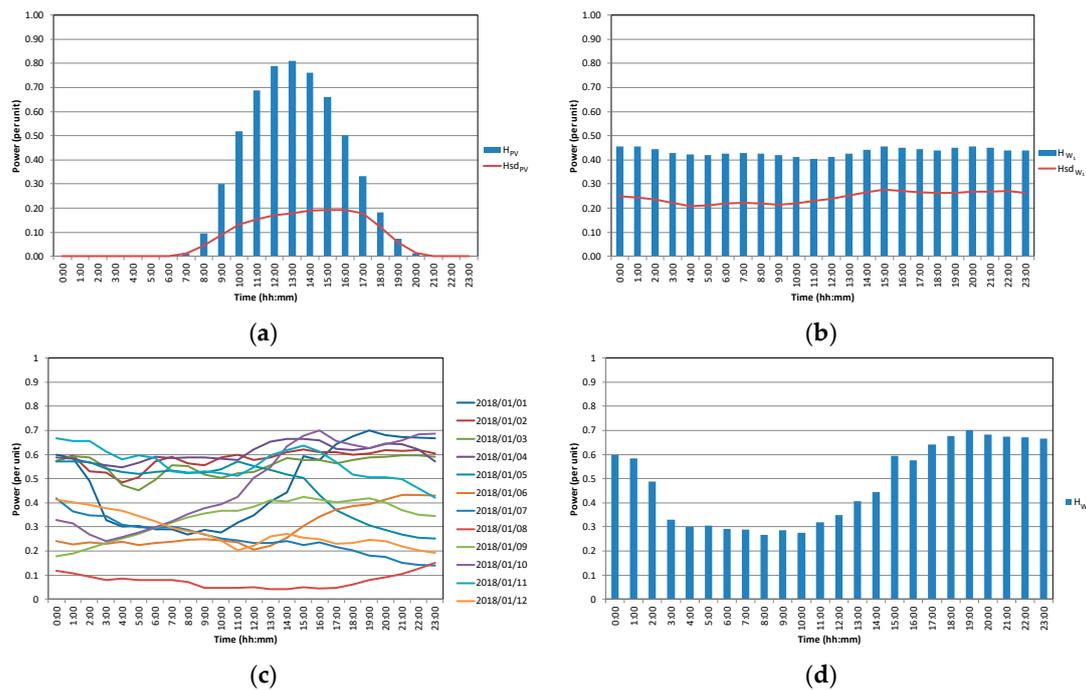
Figure 3. Generation profiles registered for the case studies. (**a**) shows the typical PV generation, (**b**) shows the average wind power generation, (**c**) shows different wind power profiles and (**d**) shows the selected wind power generation profile selected to complete this study.

3.6. Wind Generation

The average hourly active power generated during one year in the wind power plants of Spain was obtained from the Spanish system operator website [29]. In Figure 3b the average curves during the measurement campaign in per unit values H_{W_1} are represented by bars and their standard deviation is represented by a line. For this curve, an average value of $AVG_W = 0.4352$ and root mean square value $RMS_W = 0.4354$ were obtained. In this type of generator, it was assumed that it is possible to produce reactive power up to a limit of 20% of the installed power.

Figure 3c shows the curves corresponding to 12 consecutive days. Note that this type of resource has a high dispersion and its annual average curve has practically identical values at all hours. Therefore, the use of the average value would not be very realistic nor interesting to illustrate the application of the method. Thus, a random day was selected from among all the available measures to use its curve as H_W profile of availability for this plant. This profile is represented in Figure 3d.

3.7. Dispatchable Generators

This group includes plants that can regulate the generation of active and reactive power. Therefore, hydraulic, thermal, or biogas plants, among others, were included here. For this type of manageable generator, an average utilization factor of 90% was considered. It was assumed that they can produce or consume both reactive power and active power with the limit of their installed power reduced by the aforementioned utilization factor.

3.8. Case Study 1

The IEEE 30-Bus system had 30 buses with a total demand of 283.4 MW and 126.2 Mvar. The proposed method was applied after assigning demand profiles, as commented above, and the results are analyzed in Section 4. Bus 1 was the slack bus and it was considered to be connected to an infinite power grid whose generation was not limited and whose generation costs, according to Equation (1), were calculated with the values $\alpha_2 = -0.005$, $\alpha_1 = 65$, $\alpha_0 = 0$, $\beta_2 = 0.0723$, $\beta_1 = 0$.

Active power costs in the slack bus were slightly high to try to reduce the importation of energy and make use of the network's own generators. α_2 was assigned a small and negative value to represent a higher performance of the generation systems when operating close to the rated power. As for the coefficient α_1, a value close to the current price of energy exchange in Spain was used [30]. Reactive power costs were required in order to avoid having generators that only contributed Q when applying the algorithm to solve the OPF. The reactive power cost function was taken as a second-degree monomial to prevent reactive power from providing a benefit when it is negative. As mentioned in Section 3, in the slack bus, the constraint $P > 0$ must be satisfied.

The network diagram can be seen in Figure 4. The network parameters can be obtained from [31] and downloaded from [32].
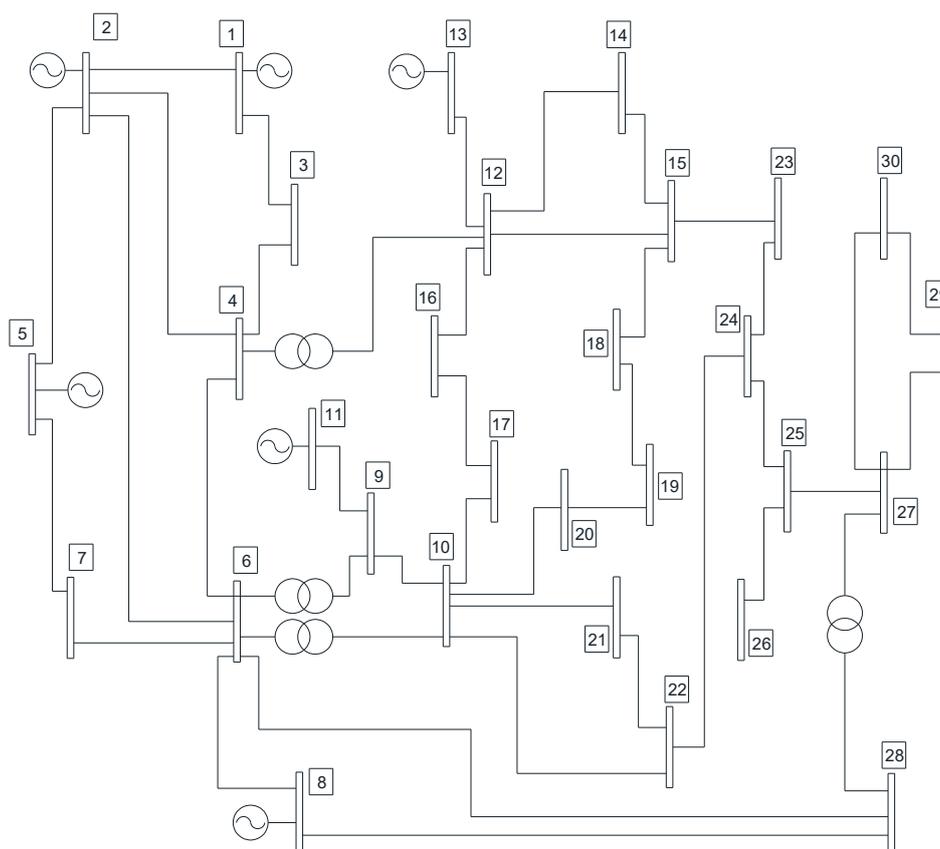
Figure 4. Diagram of the IEEE 30-Bus System.

With the curves assigned as explained, the network demand data are shown in Table 3.

The optimization of the network design by adding a group of generators according to Table 2 was proposed for this case study. This group consisted of two photovoltaic generators, two wind generators, and one manageable generator.

Table 2. Description of the new generators to be installed.

	Photovoltaic	Wind	Manageable
Power limits of each generator (MW/Mvar)	200/0	200/40	200/200
α_0 (€)	0	0	0
α_1 (€/MW)	5	10	18
α_2 (€/MW^2)	−0.005	−0.005	−0.005
β_1 (€/Mvar)	-	0	0
β_2 (€/Mvar^2)	-	0.0723	0.0723
C_a, amortization cost per hour (€/MWp/h)	7	11.4	20.6

Table 3. Demand profiles assigned in the IEEE 30-Bus System.

Bus	P_d (MWp)	Q_d (Mvarp)	Type of Consumer	Proposed Demand Profile
1-slack	0	0	-	-
2	21.7	12.7	Very large consumer	H_4
3	2.4	1.2	Small consumer	H_1
4	7.6	1.6	Large consumer	H_3
5	94.2	19	Very large consumer	H_4
6	0	0	-	-
7	22.8	10.9	Very large consumer	H_4
8	30	30	Very large consumer	H_4
9	0	0	-	-
10	5.8	2	Large consumer	H_3
11	0	0	-	-
12	11.2	7.5	Very large consumer	H_4
13	0	0	-	-
14	6.2	1.6	Large consumer	H_3
15	8.2	2.5	Large consumer	H_3
16	3.5	1.8	Medium consumer	H_2
17	9	5.8	Large consumer	H_3
18	3.2	0.9	Medium consumer	H_2
19	9.5	3.4	Large consumer	H_3
20	2.2	0.7	Small consumer	H_1
21	17.5	11.2	Very large consumer	H_4
22	0	0	-	-
23	3.2	1.6	Medium consumer	H_2
24	8.7	6.7	Large consumer	H_3
25	0	0	-	-
26	3.5	2.3	Medium consumer	H_2
27	0	0	-	-
28	0	0	-	-
29	2.4	0.9	Small consumer	H_1
30	10.6	1.9	Very large consumer	H_4

The generation costs were calculated with Equation (2) using the values indicated in Table 2 for each generator. The selected costs were approximate values obtained from real facilities and contrasted with the database available in [33]. The amortization costs of existing generators (slack) were not considered.

For the calculation of the OPF, a voltage drop limit of ±7% was imposed on all buses, in accordance with current Spanish regulations [34].

The results of applying the OGSDYP method to the described network are shown in Section 4. The discussion of these results is also shown in that section.

3.9. Case Study 2

The IEEE 118-Bus System had 118 buses with a total demand of 4242 MW and 1438 Mvar. Without loss of generality, bus 1 was considered the slack bus (bus numbers have been modified) and it was considered connected to an infinite power network whose generation was not limited and whose generation costs were considered as in case study 1.

This case study was developed to increase the complexity and analyze the convergence of the OGSDYP method based on PSO. In this case, the 54 existing generators in the network were maintained and 10 generators were added with the same proportion of each type as case study 1. In order to try to improve the convergence of the method, the evolution curve of the randomly initialized PSO was compared using a smart initialization, guided by the CE algorithm. The network data can be found in [35].

As in case study 1, all consumers were classified in categories H_1, H_2, H_3, or H_4. The proposed generation to add consisted of four photovoltaic, four wind, and two manageable generators with the parameters indicated in Table 2.

The generators to be added in each network were proposed to include generators of all types with sufficient capacity to provide the total active and reactive power demanded in the network in each scenario. In the resulting generation mix, a significant installed power of RRs was considered, which satisfied the goal of achieving a sustainable development or reinforcement of electricity grids.

The results of applying the proposed method to the described network are shown and discussed in Section 4.

4. Results and Discussion

4.1. Effectiveness and Robustness of the OGSDYP Method

The proposed method was applied to both cases using Matlab R2017b and the results and their discussion are explained in this section. To solve the OPF problems, the MATPOWER tool was used and the Matlab Optimization Toolbox was also used.

The OGSDYP method with a standard PSO algorithm was used for the 30-bus system. For the 118-bus system, the use of PSO and the use of a hybrid CE-PSO algorithm were compared. The parameters used in the simulations are shown in Table 4.

Table 4. Configuration parameters in the simulation algorithms.

Option	Description	Value
Swarm Size	Number of particles	25
Function Tolerance	The algorithm stops if after 20 stall iterations a relative change in best fitness is less than this amount	10^{-3}
Maximum Iterations	Maximum number of iterations of PSO algorithm	100
Inertia Range	Lower and upper bound of the adaptive inertia	$0.1 \div 0.9$
Self-adjustment Weight	Weighting of each particle's best position when adjusting velocity, c1	2
Social-adjustment Weight	Weighting of the neighborhood's best position when adjusting velocity, c2	2
Minimum Neighbors Fraction	Minimum adaptive neighborhood size (%)	100%
CE population	Number of particles of CE algorithm	100
CE Maximum Iterations	Maximum number of iterations of CE algorithm	4
CE Elitist Population	Percentage of elitist population of CE algorithm to generate next iteration distribution	50
CE-PSO Population Size	Number of particles for PSO after the initialization with CE	10

The most remarkable results are explained below.

4.1.1. Convergence of the Proposed Method

The convergence is the proposed method is fast during the first 20 iterations, achieving solutions very close to the optimum. The global optimum can be achieved in fewer than 100 iterations, but after

the first 20 iterations, the improvements in the objective function are very low and the convergence is very slow.

To show this, first, the generation schedule in the 30-bus network was optimized with OGSDYP by limiting the number of iterations to 100. With this simulation, the solution after 20 iterations and the final solution after convergence were compared to check that this number of iterations was a good approximation. Figure 5 shows the results of this simulation. As shown in Figure 5, the error in the objective function value after 20 iterations when compared to the final value after convergence (at 64 iterations) was €1033.83, which represents a relative error of 0.54%. Therefore, the limit of 20 iterations for a pre-design was adopted for the rest of the simulations.
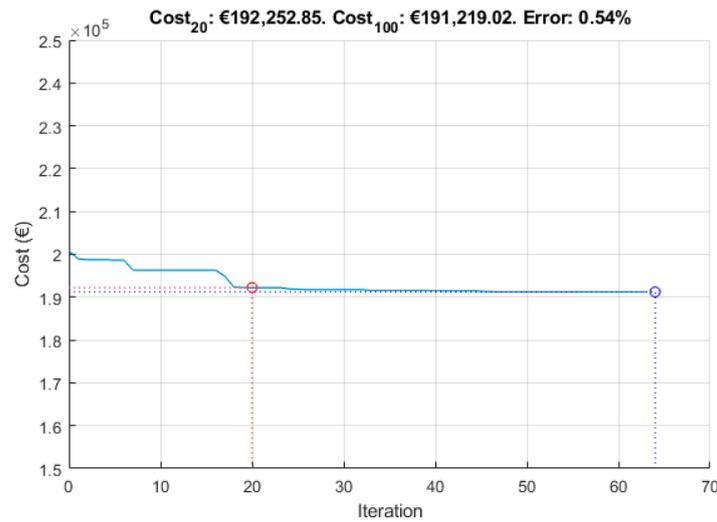
Figure 5. Evolution of the objective function value using the OGSDYP method.

In addition, in Figure 6 the optimal solutions proposed after 20 iterations and in the final convergence are compared. In this figure, PV represents photovoltaic plants, W represents wind farms, and M represents dispatchable generators. Both solutions were very similar. The differences were that some plants showed slight changes in size and others were moved to nearby buses.
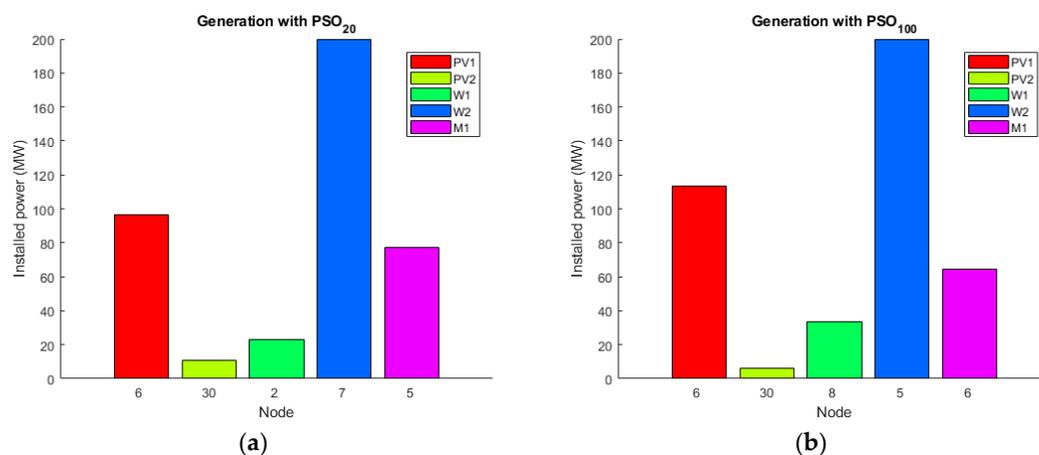
Figure 6. Solutions proposed by the OGSDYP method after 20 iterations (**a**), and after convergence in iteration 64 (**b**).

4.1.2. The Importance of Using Dynamic Profiles

It is very important to use dynamic profiles for demand and for the availability of generators. Otherwise, the obtained results lead to suboptimal schedules and the total costs of the system can be considerably higher than the optimal costs.

A very interesting analysis that was carried out was the comparison of these results with those obtained if fixed values of demand and generation were considered, like in the studies already published in the literature, instead of curves like the proposed ones. As typical characteristic parameters, AVG and root mean square (RMS) values were used, defined by Equations (25) and (26), respectively. Since the target was optimizing the cost for the whole day, AVG was a value that seemed appropriate to represent the equivalent status along it. Note that the RMS value could also be interesting since, with small variations of voltage in buses, losses in branches are proportional to the squared demand. The solutions obtained with these fixed values are shown in Figure 7. Once the solution was obtained, the actual cost was evaluated with the mentioned solution, taking into account the variation in demand and generation, which was obtained using curves to solve the OPF for the whole day. As noted, there were significant differences with the solution obtained using the OGSDYP method. Table 5 compares the three simulations. As shown in Table 5, these indicators were not very suitable to replace the curves, since the errors obtained in the costs were 9.85% for AVG and 19.46% for RMS. As regards active energy losses, the use of AVG values and RMS values to solve the OPF for all scenarios resulted in increases of 103.81% and 58.86%, respectively, compared to the OGSDYP method. In addition, it is important to make use of the curves when possible, especially if the goal is to optimize the generation to plan the network, since this decision will affect the operation for many years. This is because the optimal solution (location and size of generators), can be significantly different to the solutions obtained if demand and generation profiles are not taken into account. In this regard, Figure 7 shows that both simulations provided significantly different schedules to the solution proposed by the OGSDYP method.
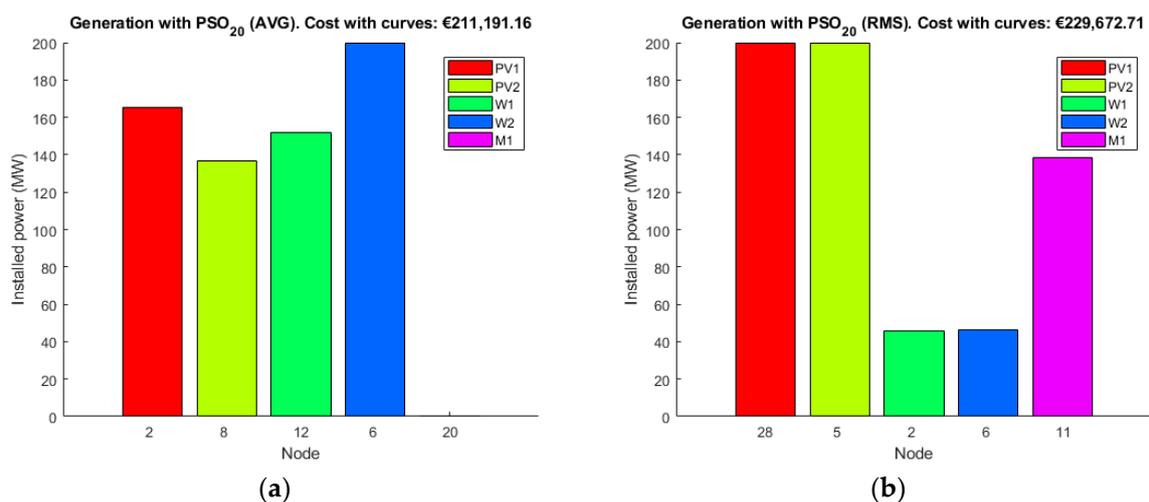

Figure 7. Solutions obtained with AVG values (**a**) and RMS values (**b**).

Table 5. Results with the OGSDYP method compared to results with AVG and RMS values.

Type of Profiles	Total Daily Cost (€)	Cost Difference Compared to the Use of Curves (%)	Total Daily Demand (MWh)	Total Daily Active Energy Generation (MWh)	Total Daily Losses (MWh)	Losses Difference Compared to the Use of Curves (%)
Curves	192,252.85	0	4818.08	4,864.61	46.53	0
AVG	211,191.16	9.85	4818.08	4912.91	94.83	103.81
RMS	229,672.71	19.46	4818.08	4892.00	73.92	58.86

As shown in Table 5, the use of dynamic profiles can represent great improvements both in the total generation costs and in the system losses. This highlights one of the most important advantages of the OGSDYP method compared to most previously published works, which used fixed values for generation and demand.

4.1.3. Diversity of Demand

The use of demand profiles must reflect the reality of the grid operation. If a single profile is used in all buses, the results will not be optimal.

In order to provide a more detailed analysis, the method was compared with some works that used the same load profile in every bus. If the optimization algorithm was applied assigning the same profile to all buses, for example, considering all nodes as large consumers with a profile H_3, the optimal solution would be the generation schedule shown in Figure 8.
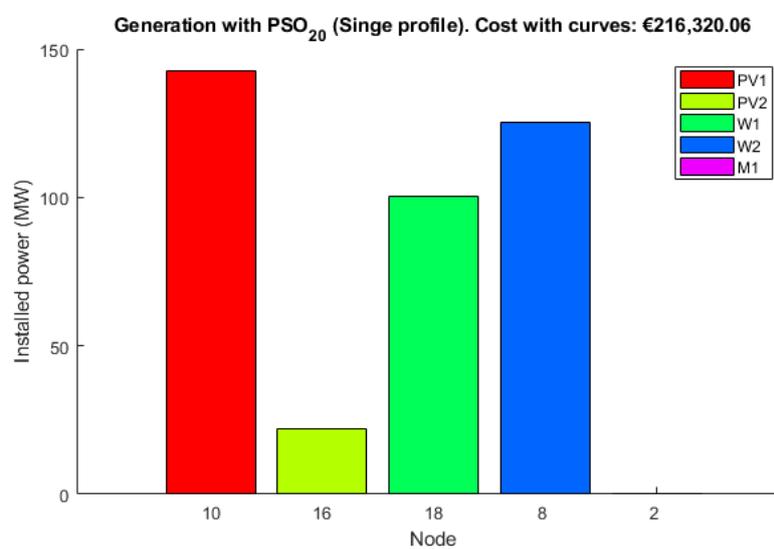
Figure 8. Solution obtained considering all nodes as large consumers.

The solution was more similar to the one obtained with AVG values than to the one obtained with dynamic profiles. With this solution, the total cost computed with the demand profiles assigned in this case study was €216,320.06, which is 12.52% higher than the optimal costs provided be the OGSDYP method. This result shows the importance of considering different profiles in every bus as a better approach of the reality of the network operation conditions.

In addition to studying the improvement provided by the OGSDYP method, a robustness analysis was made by repeating the simulation 50 times to verify the reliability of the results after 20 iterations. Figure 9 shows the box plot that represents the distribution of the solutions obtained through OGSDYP and with fixed AVG and RMS values. The solutions obtained with the proposed method showed very low dispersion and substantially lower costs than the solutions obtained with fixed values.
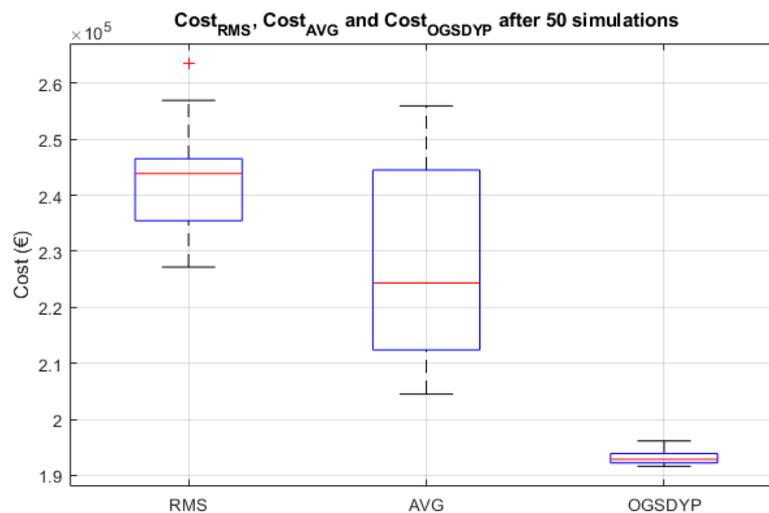
Figure 9. Distribution of the costs obtained with RMS values, AVG values, and the OGSDYP method after 20 iterations.

4.1.4. Consistency of the Optimal Solution

The solution obtained with the OGSDYP method was consistent, since it enabled a better usage of the generators than other solutions. This solution provided better voltage values in the different buses along the typical day and lower losses than other solutions.

The proposed method achieved the best solutions for generation planning or reinforcement in electricity networks from a technical and economical point of view. Its impact is especially important for the sustainable development of generation in electricity networks, since most RRs have high variability, which strongly increases the benefits of considering dynamic profiles. Nevertheless, to show other advantages of the optimal solution obtained with the OGSDYP method, the evolution of the voltages in all buses throughout the typical day was analyzed. Similarly, the generation of active and reactive power of all generators (including the slack bus) were studied throughout the day. The results are shown in Figure 10. It must be noted that there were significant variations from one moment to another in some buses' voltage. This highlights, once again, the importance of making use of curves instead of fixed values for demand and generation, to ensure the reliability of the proposed planning over time. Specifically, buses 1, 5, 7, and 30 showed voltage variations close to 4% throughout the day.

It is also important to note that there were several power plants whose minimum generation value was greater than zero, as shown in Figure 10. This means that these plants were used throughout the day, in every moment.

These same network results are shown in Figure 11 for the solution obtained using the RMS value.

First, it must be noted that with this planning approach, the voltage of most buses showed much greater variations throughout the day. Therefore, the voltages profile of the network was clearly worse. This is due to the fact that the evolution of the operation throughout the day was not optimized in the planning process, with the use of fixed values. In addition, all plants had minimum values of null active power generation, which means that they all had time intervals in the day in which they were not used. All this shows that the solution was far less optimized.

(**a**)

(**b**)

(**c**)

(**d**)
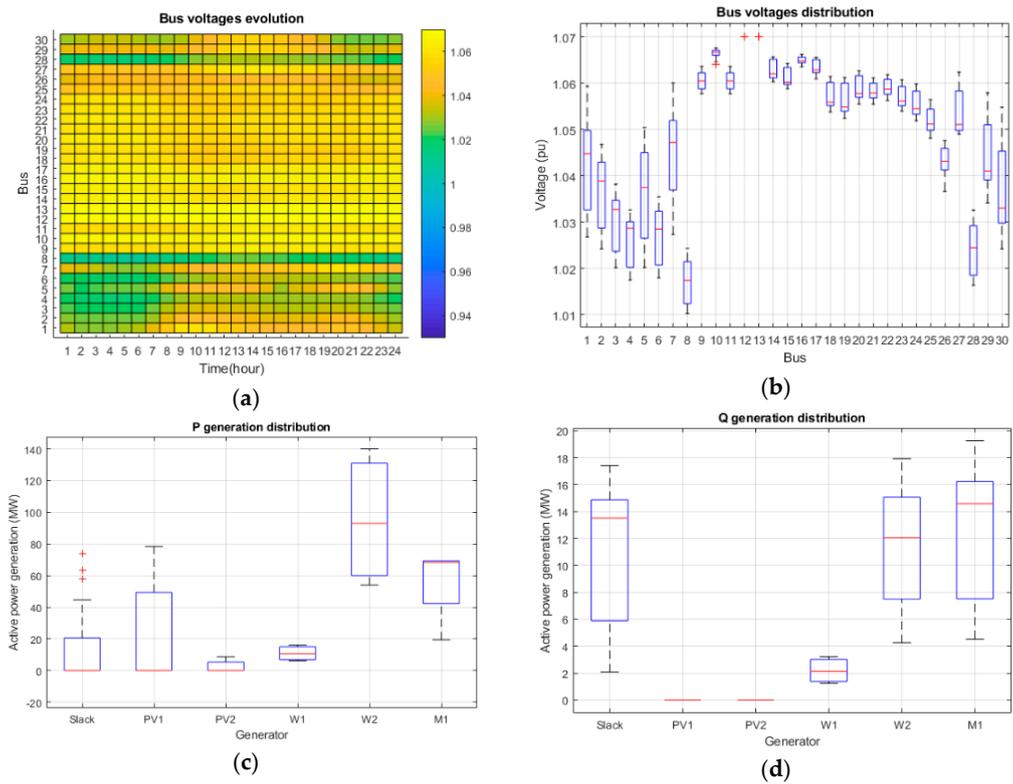
Figure 10. Evolution of voltages in all buses (**a**), distribution of voltages (**b**), generated active powers in all generators (**c**), and generated reactive powers (**d**) using the OGSDYP method.

(**a**)

(**b**)

(**c**)

(**d**)
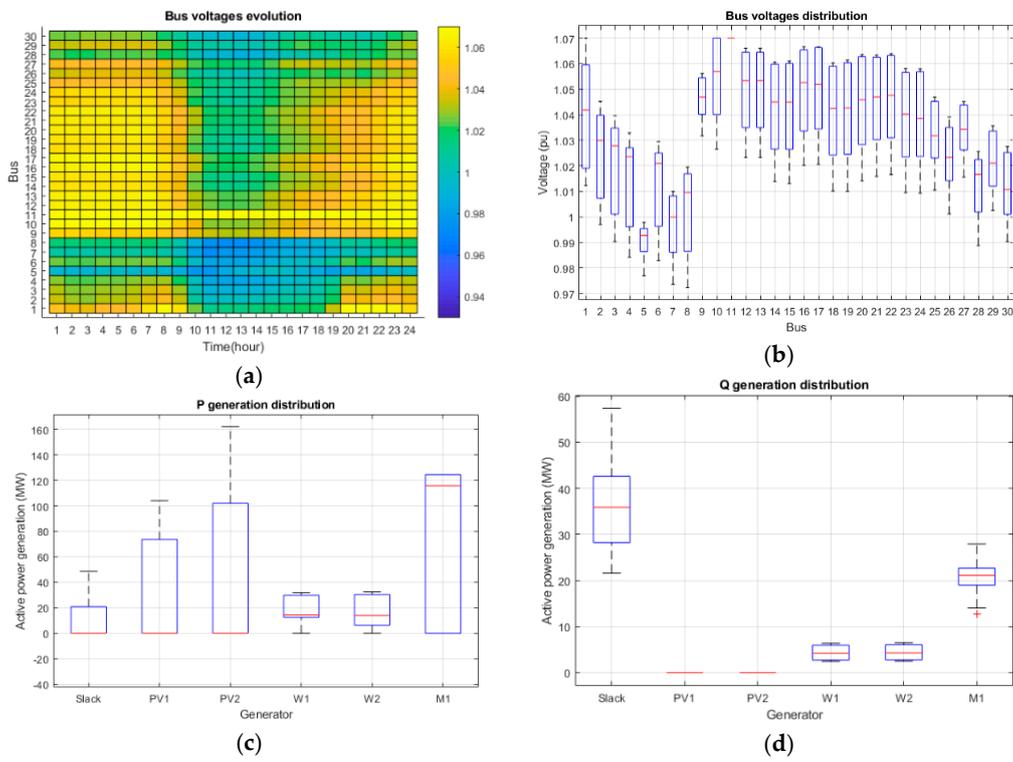
Figure 11. Evolution of voltages in all buses (**a**), distribution of voltages (**b**), generated active powers in all generators (**c**), and generated reactive powers (**d**) using RMS values.

4.2. Improvement of Convergence

After completing the analysis of the 30-bus network, the simulation was repeated with the 118-bus network to study the behavior of the OGSDYP method with problems of great complexity. The algorithm showed a good performance and provided better solutions than those obtained with fixed values for demand and generation. However, in this problem, the computational cost was considerably higher and the simulation was substantially longer. Therefore, it is interesting to search for strategies to accelerate convergence and reach approximate solutions with about 20 iterations, in order to obtain valid results for a pre-design stage. That is why in this work the authors explored the hybrid CE-PSO method based on performing four CE iterations to obtain an initial population for PSO that was not completely random. Taking into account the operation of CE, these four iterations performed a random sampling process to explore the search space of feasible solutions and they provided a subset of values with a higher probability of being close to the optimum. Therefore, the application of PSO with this initial subset tried to prevent the method from using particles with a low probability of being adequate for the optimization process.

The choice of four iterations was proposed through a trial-and-error approach by repeating the simulation with a number of iterations between 1 and 10 and analyzing the results. Figure 12 shows the evolution of the average objective function along 10 iterations of CE after repeating the experiment five times and representing mean values in each iteration. In Figure 12, the dotted line represents the number of objective function evaluations using 20 iterations of PSO with 25 particles and the continuous line represents the number of evaluations of the initialization process using CE with 100 particles. After analyzing Figure 12, four iterations of CE seems to be a good choice. It was proven that the results with four iterations presented a marked improvement with little increase in simulation time, while for five or more simulations the increase in simulation time was truly significant. On the other hand, the use of fewer than four iterations had little effect on convergence.
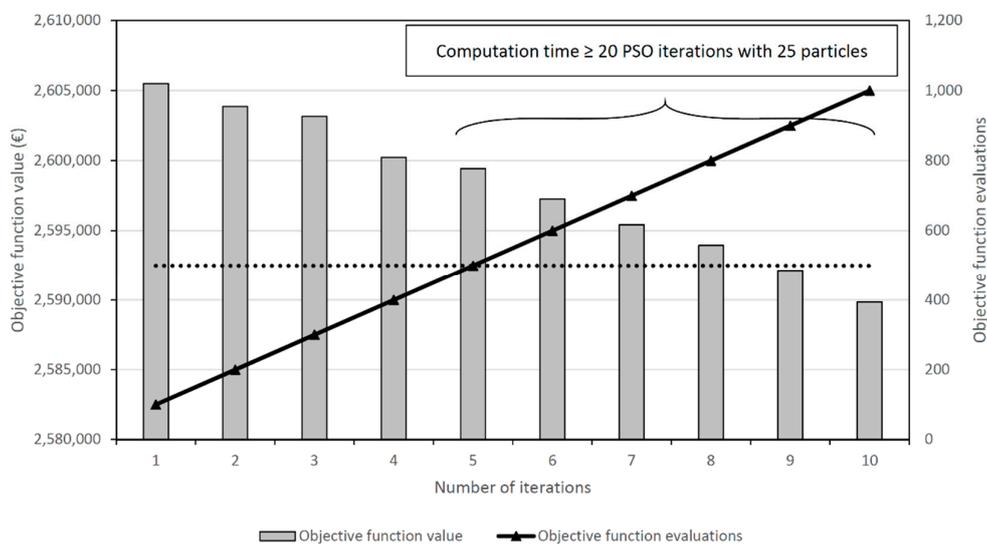

Figure 12. Evolution of the average objective function value using CE.

Figure 13 shows the results of CE-PSO algorithm compared to the PSO algorithm when applying the OGSDYP method to this case study. As depicted in Figure 13, in this case, convergence was better with the proposed method using a CE-guided initialization, since the initial PSO population was closer to the optimal solution. As of the third iteration of PSO in this simulation with the hybrid CE-PSO algorithm, all the results were better than those achieved by PSO exclusively, even after 20 iterations. Note that four iterations of CE with 100 particles plus three of PSO with 10 particles represent 430 evaluations of the objective function, and the result was better than with 20 iterations of PSO with 25

particles (500 evaluations). Just to show the differences in the design schedules at that point, Figure 14 shows the solution of the 20th iteration using both algorithms.
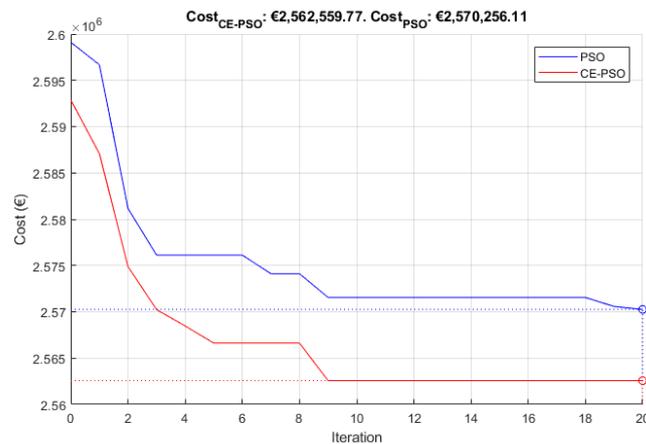

Figure 13. Evolution of the objective function value using the OGSDYP method with PSO and CE-PSO algorithms.
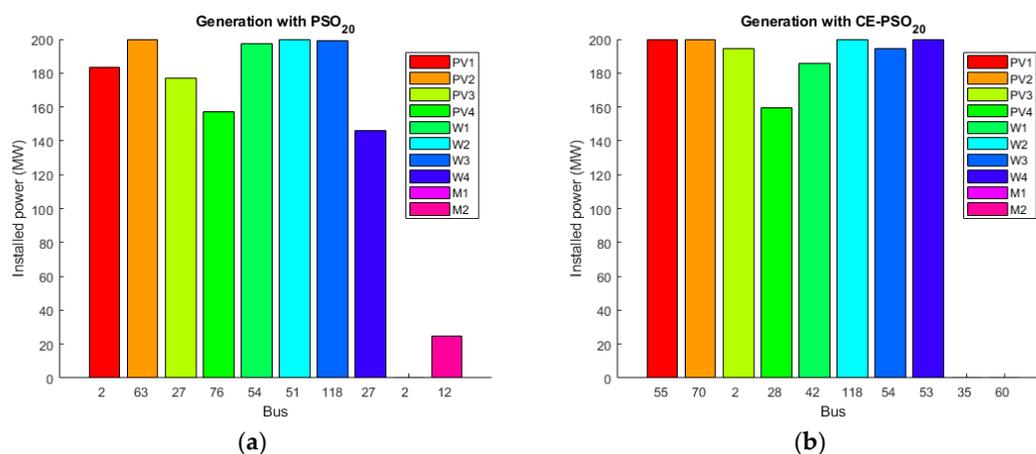

Figure 14. Solutions by iteration 20 using the OGSDYP method with PSO (**a**) and CE-PSO (**b**) algorithms.

This simulation was repeated 20 times, and 60% of the times, the result with CE-PSO was better than the results using PSO. It must be noted that with CE-PSO, after 10 iterations of PSO there were very low variations in the objective function. This could allow a reduction of the number of iterations of PSO to achieve results that are good enough for a quick pre-design. Nonetheless, more detailed simulations are needed to study the best strategy and parameters to achieve clear and reliable improvements.

In this case study, initialization with CE led to faster convergence than a random population. However, although the initialization by CE manages to focus the initial population of PSO around lower objective function values, due to the randomness of both methods and the complexity of the problem, it cannot be ensured that convergence will always be better with the hybrid CE-PSO algorithm. The obtained results were not conclusive in this aspect and more research is needed. The OGSDYP method achieved the optimal solution after some computational time, but it would be interesting to develop future research on strategies to improve convergence in such complex cases. This would enable quick simulations to provide approximate pre-designs for feasibility studies.

Future Research

The hybrid algorithm CE-PSO could be improved with more detailed studies. Studying the optimal parameters of CE (number of particles, elitist population ratio, and so on) as well as analyzing

possible modifications of PSO to take advantage of the guided initialization (number of particles, adjustment weights, inertia, and so on) should be the next steps to improve convergence for quick pre-designs in complex cases. This could enable a reduction of the number of iterations needed to achieve low errors in the final results for those quick studies. Other possible strategies for these cases could be the use of parallel computing to increase simulation speed by taking advantage of modern Central Processing Units (CPUs) with multiple cores.

5. Conclusions

This paper addressed the problem of the optimal location of generators in a power grid, their appropriate size, and operating strategy, to achieve the lowest possible generation costs. The problem was studied by considering dynamic generation and demand profiles to find the optimal global solution.

On the one hand, the economic impact that an inadequate design of the set of generators can have is significant, since it produces an increase in energy prices that could be avoided with a better design. On the other hand, a correct design of the generation systems reduces energy losses and their associated emissions. Moreover, the consideration of renewable power plants in the design process (as is this paper) favors the optimal integration of these energy sources into existing networks. All these objectives contribute to the design of more sustainable networks for the future.

In many countries with unregulated energy markets, the purchase price of energy does not depend on the injection buses of the grid. However, this practice leads to inappropriate designs and higher prices for consumers. The proposed algorithm provides the optimal location and size of new generation facilities in the network. In addition, it is possible to study the effect of a power plant at a specific location. This could be done by including it as an existing generator, and assessing the difference in the generation cost between the original network and a proposed alternative. In power systems, the installation of new power plants in the optimal buses of the network should be enhanced with discounts on energy prices, compared to other buses, where the installation of these power plants can produce a lower benefit in the system operation. This would enhance a better development that could allow a reduction in energy losses (and associated greenhouse gas emissions) and a more sustainable design.

The algorithm presented in this paper was designed to determine the ideal buses for installing new power plants, depending on their type. It also provides the optimum power to install for each of them. Likewise, the algorithm shows the optimal operation strategy of all power plants in the network, both new and existing ones, facilitating the network operation scheduling. To the knowledge of the authors, no algorithm proposed so far has all these features. Taking into account the need to reinforce networks' generation with RRs to achieve more sustainable scenarios, the cases studied in this work have focused on the installation of renewable power plants (photovoltaic, wind, biogas) in existing networks. Since these types of plants are not manageable in most cases, it was necessary to take into account, in the optimal design, the availability curves of these generators. To optimize the network with dynamic generation profiles, it was also necessary to take into account demand variations. Therefore, the algorithm can be applied with generation and demand profiles that can be entered either individually or by grouping the elements into clusters. In the developed case studies, four types of demand profiles and three types of generation profiles based on real data were used. Nonetheless, individual data could be used for every element, if they were available. This represents an important novelty of this algorithm compared to others proposed in the literature.

Another remarkable feature of the proposed algorithm is that specific costs can be assigned to each generating plant if this information is available. In the case studies, different costs have been assigned according to the type of plant (photovoltaic, wind, biogas), but individualized costs can also be used, since the algorithm queries the cost for each generator during its execution.

The method was tested in detail in a standard network with 30 buses and some simulations were also applied to another standard network with 118 buses. As regards the case studies developed in this work, it should be highlighted that the generation designs made without taking into account the

dynamic evolution of demand and generation (for example, using average values) produced results substantially worse than the optimal values. When analyzing these results, significant increases in total generation costs and energy losses were observed. For example, in case study 1, the design of the generation based on average power values in the buses led to a solution whose generation costs were 9.85% higher than the optimal solution obtained with dynamic power profiles. As for the losses, these increased by 103.81% with respect to the optimal case. Additionally, the operation of the grid with designs carried out with fixed values showed lower stability in voltages and a worse usage of resources.

In many literature works, renewable generation is used for DG with small-sized plants, which is applicable to small distribution networks. However, currently, wind farms reach very high power and are usually connected to transmission networks. In addition, the size of photovoltaic power plants is increasing and they are already at powers of hundreds of megawatts, as well as the thermal solar power plants, so these new power plants are also connected to transmission networks. Thus, it is necessary to study the consequences that these plants could have in order to guarantee the optimal operation of these large networks. In this regard, it should be noted that the algorithm can be applied to both small networks (microgrids, distribution networks) and large networks (transmission networks) with the only limitation of the computing costs. This is justified for two reasons. On the one hand, the OPF algorithm used in this work is of general application to any grid. On the other hand, in large networks, the availability curves of plants can be particularized. This means that these curves can be adjusted to the climatic parameters of each location.

Additionally, as a starting point for future research, this paper proposed the use of CE to generate the initial population for PSO for large networks. This strategy seems to lead to better results with fewer iterations, although the results are not conclusive. It may be interesting to study a smart control of a hybrid CE-PSO method in order to reduce the computational cost of these complex problems.

References

1. Höök, M.; Tang, X. Depletion of fossil fuels and anthropogenic climate change—A review. *Energy Policy* **2013**, *52*, 797–809. [CrossRef]
2. Van de Ven, D.J.; Fouquet, R. Historical energy price shocks and their changing effects on the economy. *Energy Econ.* **2017**, *62*, 204–216. [CrossRef]
3. Osório, G.J.; Shafie-khah, M.; Lujano-Rojas, J.M.; Catalão, J.P.S. Scheduling Model for Renewable Energy Sources Integration in an Insular Power System. *Energies* **2018**, *11*, 144. [CrossRef]
4. Lasseter, R.H. Smart distribution: Coupled microgrids. *Proc. IEEE* **2011**, *99*, 1074–1082. [CrossRef]
5. Moriarty, P.; Honnery, D. Can renewable energy power the future? *Energy Policy* **2016**, *93*, 3–7. [CrossRef]
6. Ghosh, S.; Ghoshal, S.P.; Ghosh, S. Optimal sizing and placement of distributed generation in a network system. *Int. J. Electr. Power Energy Syst.* **2010**, *32*, 849–856. [CrossRef]
7. Gomez-Gonzalez, M.; López, A.; Jurado, F. Optimization of distributed generation systems using a new discrete PSO and OPF. *Electr. Power Syst. Res.* **2012**, *84*, 174–180. [CrossRef]

8. Li, Y.; Li, Y.; Li, G.; Zhao, D.; Chen, C. Two-stage multi-objective OPF for AC/DC grids with VSC-HVDC: Incorporating decisions analysis into optimization process. *Energy* **2018**, *147*, 286–296. [CrossRef]

9. Krueasuk, W.; Ongsakul, W. Optimal Placement of Distributed Generation Using Particle Swarm Optimization. In Proceedings of the Australasian Universities Power Engineering Conference (AUPEC) 2006, Melbourne, Australia, 10–13 December 2006; pp. 1–6.

10. Yassine, A.A.; Mostafa, O.; Browning, T.R. Scheduling multiple, resource-constrained, iterative, product development projects with genetic algorithms. *Comput. Ind. Eng.* **2017**, *107*, 39–56. [CrossRef]

11. Dias, B.H.; Oliveira, L.W.; Gomes, F.V.; Silva, I.C.; Oliveira, E.J. "Hybrid heuristic optimization approach for optimal Distributed Generation placement and sizing". In Proceedings of the 2012 IEEE Power and Energy Society General Meeting, San Diego, CA, USA, 22–26 July 2012; pp. 1–6. [CrossRef]

12. Silvestri, A.; Berizzi, A.; Buonanno, S. Distributed generation planning using genetic algorithms. In Proceedings of the PowerTech Budapest 99. Abstract Records. (Cat. No.99EX376), Budapest, Hungary, 29 August–2 September 1999; p. 257.

13. Prakash, D.B.; Lakshminarayana, C. Multiple DG Placements in Distribution System for Power Loss Reduction Using PSO Algorithm. *Procedia Technol.* **2016**, *25*, 785–792. [CrossRef]

14. Mithulananthan, N.; Oo, T. Distributed generator placement in power distribution system using genetic algorithm to reduce losses. *Sci. Technol. Asia* **2004**, *9*, 55–62.

15. Niknam, T.; Ranjbar, A.M.; Shirani, A.R.; Mozafari, B.; Ostadi, A. Optimal operation of distribution system with regard to distributed generation: A comparison of evolutionary methods. In Proceedings of the Fourtieth IAS Annual Meeting. Conference Record of the 2005 Industry Applications Conference, Kowloon, Hong Kong, China, 2–6 October 2005; pp. 2690–2697.

16. Kim, K.H.; Lee, Y.J.; Rhee, S.B.; Lee, S.K.; You, S.K. Dispersed generator placement using fuzzy-GA in distribution systems. In Proceedings of the IEEE Power Engineering Society Summer Meeting, Chicago, IL, USA, 21–25 July 2002; Volume 3, pp. 1148–1153.

17. Hung, D.Q.; Mithulananthan, N.; Bansal, R.C. Analytical strategies for renewable distributed generation integration considering energy loss minimization. *Appl. Energy* **2013**, *105*, 75–85. [CrossRef]

18. Syahputra, R.; Robandi, I.; Ashari, M. Reconfiguration of Distribution Network with Distributed Energy Resources Integration Using PSO Algorithm. *Telkomnika* **2015**, *13*, 759–766. [CrossRef]

19. Ueckerdt, F.; Brecha, R.; Luderer, G. Analyzing major challenges of wind and solar variability in power systems. *Renew. Energy* **2015**, *81*, 1–10. [CrossRef]

20. Kansal, S.; Kumar, V.; Tyagi, B. Optimal placement of different type of DG sources in distribution networks. *Int. J. Electr. Power Energy Syst.* **2013**, *53*, 752–760. [CrossRef]

21. De Magalhães Carvalho, L.; da Silva, A.M.; Miranda, V. Security-Constrained Optimal Power Flow via Cross-Entropy Method. *IEEE Trans. Power Syst.* **2018**, *33*, 6621–6629. [CrossRef]

22. Yadav, V.; Ghoshal, S.P. Optimal power flow for IEEE 30 and 118-bus systems using Monarch Butterfly optimization. In Proceedings of the 2018 Technologies for Smart-City Energy Security and Power (ICSESP), Bhubaneswar, India, 28–30 March 2018; pp. 1–6.

23. Zimmerman, R.D.; Murillo-Sánchez, C.E.; Thomas, R.J. MATPOWER: Steady-State Operations, Planning, and Analysis Tools for Power Systems Research and Education. *IEEE Trans. Power Syst.* **2011**, *26*, 12–19. [CrossRef]

24. Zimmerman, R.D.; Murillo-Sanchez, C.E. Matpower 7.0 User's Manual; PSERC, USA. 2019. Available online: https://matpower.org/docs/manual.pdf (accessed on 6 November 2019).

25. Wang, H.; Murillo-Sanchez, C.E.; Zimmerman, R.D.; Thomas, R.J. On Computational Issues of Market-Based Optimal Power Flow. *IEEE Trans. Power Syst.* **2007**, *22*, 1185–1193. [CrossRef]

26. Wang, H. On the Computation and Application of Multi-Period Security-Constrained Optimal Power Flow for Real-Time Electricity Market Operations. Ph.D. Thesis, Cornell University, Ithaca, NY, USA, 2007.

27. Abdi, H.; Beigvand, S.D.; Scala, M.L. A review of optimal power flow studies applied to smart grids and microgrids. *Renew. Sustain. Energy Rev.* **2013**, *71*, 742–766. [CrossRef]

28. Rubinstein, R.Y.; Kroese, D.P. *The Cross-Entropy Method: A Unified Approach to Combinatorial Optimization, Monte-Carlo Simulation and Machine Learning*; Springer: New York, NY, USA, 2004.

29. Red Eléctrica de España. Available online: http://www.ree.es (accessed on 6 November 2019).

30. OMIE. Operador del Mercado Ibérico-Polo Español S.A. Available online: http://www.omie.es (accessed on 6 November 2019).

31. Alsac, O.; Stott, B. Optimal Load Flow with Steady-State Security. *IEEE Trans. Power Appar. Syst.* **1974**, *PAS-93*, 745–751. [CrossRef]
32. The IEEE 30-Bus Test System. Available online: https://labs.ece.uw.edu/pstca/pf30/pg_tca30bus.htm (accessed on 6 November 2019).
33. Open Energy Information—Transparent Cost Database. Available online: https://openei.org/apps/TCDB/ (accessed on 6 November 2019).
34. Boletín Oficial del Estado. Real Decreto 1955/2000, de 1 de Diciembre, Por el Que se Regulan las Actividades de Transporte, Distribución, Comercialización, Suministro y Procedimientos de Autorización de Instalaciones de Energía Eléctrica, (in Spanish). 2000. Available online: https://www.boe.es/boe/dias/2000/12/27/pdfs/A45988-46040.pdf (accessed on 6 November 2019).
35. The IEEE 118-Bus Test System. Available online: https://labs.ece.uw.edu/pstca/pf118/pg_tca118bus.htm (accessed on 6 November 2019).